2022

Experimental Investigation of Additively Manufactured Microchannel Evaporator Performance Using Low-GWP Refrigerants Compared to Conventional Air Cooling in Electronics Cooling

Theresa Kramer

Kevin Lemberg

Riley B. Barta

Mario Raddatz

Ullrich Hesse

Experimental Investigation of Additively Manufactured Microchannel Evaporator Performance Using Low-GWP Refrigerants Compared to Conventional Air Cooling in Electronics Cooling

Theresa KRAMER*[1], Kevin LEMBERG[2], Riley B. BARTA[1], Mario RADDATZ[2], Ullrich HESSE[1]

[1]Technische Universität Dresden, BITZER-Chair of Refrigeration, Cryogenics and Compressor Technology,
Dresden, Saxony, Germany
theresa.kramer@tu-dresden.de
riley.barta@tu-dresden.de
ullrich.hesse@tu-dresden.de

[2]Technische Universität Dresden, Chair of Thermal Power Machinery and Plants,
Dresden, Saxony, Germany
kevin.lemberg@tu-dresden.de
mario.raddatz@tu-dresden.de
* Corresponding Author

ABSTRACT

With the increasing electrification of power systems, the need for efficient energy conversion systems and hereby power electronics increases correspondingly. Power semiconductor devices such as diodes, power transistors, or thyristors enable an efficient conversion or switching of electricity from a few milliwatts up to nearly a gigawatt. Typical power semiconductor devices include components from the group of MOSFET (*Metal Oxide Semiconductor Field Effect Transistor*), GTO- (Gate Turn Off-) Thyristors, IGCT (*Integrated Gate Commutated Thyristor*), power diodes and especially IGBT (*Insulated Gate Bipolar Transistor*). These Semiconductor components are decreasing in size while increasing in power and capacity. Therefore, novel efficient cooling strategies are growing in importance and relevance.
Until now over 95 % of industrial applications from the stationary and mobile sectors use cooling concepts based on conventional air or liquid cooling. Although liquid and air cooling are already quite developed and tested, two-phase cooling could increase the heat transfer coefficient as well as the amount of heat absorbed, and could therefore help cooling semiconductor components with their associated increasing power and decreasing size.
In this paper, the potential of evaporative cooling in microchannel heat exchangers for power electronics cooling applications is examined. It is shown that, through the usage of additively manufactured microchannel heat exchangers instead of conventional air cooling, the absorbed heat flux can be more than doubled.

1. INTRODUCTION

The semiconductor device IGBT (*Insulated Gate Bipolar Transistor)* is of particular importance for power electronics in most industries. Therefore, the IGBT is taken as reference for a typical semiconductor device. An essential development goal of the IGBT is the increase of the acceptable junction temperature ϑ_{SF}. In the last years the acceptable junction temperature has increased from 125 °C to 150 °C (Noriyuki Iwamuro & Thomas Laska, 2017), (Lubin Han et al., 2021).

The conventional cooling of an IGBT is mostly realised through a so-called cold plate, which is mounted directly on top of the IGBT. Cooling via evaporation of refrigerants in heat exchangers directly at the surface of the active elements theoretically improves heat transfer and reduces the required surface and specific weight of the heat exchangers. However, challenges associated with two-phase cooling are the reliable control in all operating conditions as well as a safe integration into existing system architectures. In particular, microchannel heat exchangers pose a challenge when it comes to simulation, calculation and design.

Microchannel heat exchangers have a substantial potential for applications in systems where available weight and size is limited. However, the flow behaviour differs greatly from that of a macrochannel. The transition from a conventional macrochannel to a microchannel can be described by various criteria including the hydraulic diameter d_h, the Knudsen number Kn, the confinement number Co and the bubble diameter d_B. One typical definition according to Kandlikar is as follows (Satish G. Kandlikar, 2002):

- Microchannel: $10\mu\mathrm{m} \leq d_\mathrm{h} \leq 200\ \mu\mathrm{m}$
- Minichannel: $200\mu\mathrm{m} \leq d_\mathrm{h} \leq 3\ \mathrm{mm}$
- Macrochannel: $d_\mathrm{h} \geq 3\ \mathrm{mm}$

A distinction between mini- and microchannel-based systems should be made because of phenomenological and practical reasons. For example, the bubble ebullition processes that follow bubble nucleation in microchannels differ from those in minichannels. (S. Mostafa Ghiaasiaan, 2007)

Nevertheless, in this paper mini- and microchannels will not be differentiated. Instead, all channels with $d_\mathrm{h} \leq 3\ \mathrm{mm}$ will be called microchannel. The maximum heat transfer coefficient of a typical coldplate with one-phase fluid flow is approximately $\alpha = 10{,}000\ \mathrm{W/(m^2K)}$ (B. Jayant Baliga, 2015). On the other hand, a state-of-the-art IGBT-module has a local heat transfer rate of up to $50\ \mathrm{MW/m^2}$ (T. G. Karayiannis & M. M. Mahmoud, 2017). Therefore, new cooling techniques have to be developed if reasonable temperature gradients are to be maintained. Through the definition of the heat transfer coefficient α according to equation (1) one can see, that the heat transfer will increase with decreasing hydraulic diameter, thus making the microchannel heat exchanger an interesting subject.

$$\alpha = \frac{\lambda \cdot \mathrm{Nu}}{d_\mathrm{h}} \tag{1}$$

Here in λ is the thermal conductivity of the cooling fluid. The Nusselt number Nu of a one-phase fluid in a microchannel heat exchanger is mostly constant, since the flow can be assumed to be laminar. Consequently, in theory the heat transfer coefficient can be increased by solely decreasing the hydraulic diameter. One possible way of evaluating the efficiency of a compact heat exchanger is the frequently used compactness performance factor γ (Eric M Smith, 2005), which can be calculated using equation (2).

$$\gamma = \frac{\dot{Q}}{V \cdot \Delta\vartheta_\mathrm{log}} \tag{2}$$

The compactness performance factor is composed of the ratio of the transferred heat flow rate $\dot{Q}$ to the product of the heat exchanger volume and the logarithmic temperature difference $V \cdot \Delta\vartheta_\mathrm{log}$.

The use of one-phase fluids in microchannels already increases the achievable heat flux in comparison to macrochannel heat exchangers. However, using two-phase fluids increases this heat flux even further while maintaining a constant temperature at small flow rates. Due to the constant temperature, the thermal tensions inside of the power electronics device can be minimized. This paper analyzes the additive manufacturing of microchannel heat exchangers and determines the amount of heat transferred by a two-phase fluid in comparison to a one-phase fluid.

The type of evaporation and the flow behaviour are crucial for the stability and the height of the heat flux. Various previous research projects have concluded the type of evaporation and the flow behavior in microchannels are different to those in a macrochannel. In contrast to microchannels, correlations for calculating the heat transfer coefficient and pressure loss can depict the physical processes in macrochannels with sufficient accuracy (Alexander Raabe, 2021). Therefore, further measurements are necessary to characterize the flow of two-phase fluids especially in microchannels.

No correlation has been able to represent large data sets of heat transfer coefficients with sufficient accuracy. Reasons for the large differences between correlations and datasets are, on the one hand, the occurrence of extremely low liquid Reynolds numbers Re_l, which are in the laminar range, and, on the other hand, the differences in the boiling flow regime in macro- and microchannels. (S. Mostafa Ghiaasiaan, 2007)

Ultimately, further investigations regarding two-phase fluids and their potential, especially in microchannels and for application areas of growing importance like power electronics, have to be investigated. This paper presents ways of manufacturing microchannel heat exchangers additively as well as the construction of a suitable test stand to determine the heat transfer properties of the heat exchangers. The results of measurements with a two-phase fluid and with air are presented and the improvement through the two-phase fluid and different channel geometries are evaluated.

2. EXPERIMENTAL SETUP

2.1 Additive manufacturing of heat exchangers

A widely known and used process for microchannel manufacturing is the printed circuit heat exchanger manufacturing. These heat exchangers are composed of several plates by means of diffusion welding (Kuppan Thulukkanam, 2013). However, a major disadvantage of these printing technologies is the fact that, due to the process, primarily drop-shaped semicircular channels can be imaged. Even if various technologies already exist today with which varying channel cross-sections, such as trapezoidal or triangular-like channels, can be realized to some extent, the limits of the printing process for the production of micro and mini channels are foreseeable, which means that the need for new, disruptive technologies is constantly increasing. Therefore, additive manufacturing methods are being developed and researched with a greater variety of geometries that can be tested. Nowadays, additive manufacturing processes include a large selection of innovative manufacturing methods that differ fundamentally from conventional manufacturing processes. Components are not manufactured by removing material as usual, but are built up layer by layer. While there have been countless theoretical investigations and considerations on novel heat exchanger structures over the past decades, which could only be investigated numerically due to a lack of manufacturing technologies, the corresponding tools for experimental verification now exist for the first time. (K. Lemberg, T. Kramer, M. Raddatz & R. Barta, 2021)

In the present project, selective laser melting was selected as the additive manufacturing process for the heat exchangers. In the case of selective laser melting (SLM), granulate is accumulated in a powder bed to form individual layers with a typical layer thickness of 20 µm to 100 µm (Dirk Herzog et al., 2016). Figure 1 shows the result of the designed heat exchanger. The heat exchanger is inspired by the described cold plate, which is directly flanged to an IGBT-module. This is a plate measuring 125 x 50 x 5 mm³ with a total of 16 equidistantly arranged mini-channels. These plates were printed in the vertical position as shown, eliminating overhangs altogether and reducing machine costs by arranging multiple plates in parallel within a single batch.

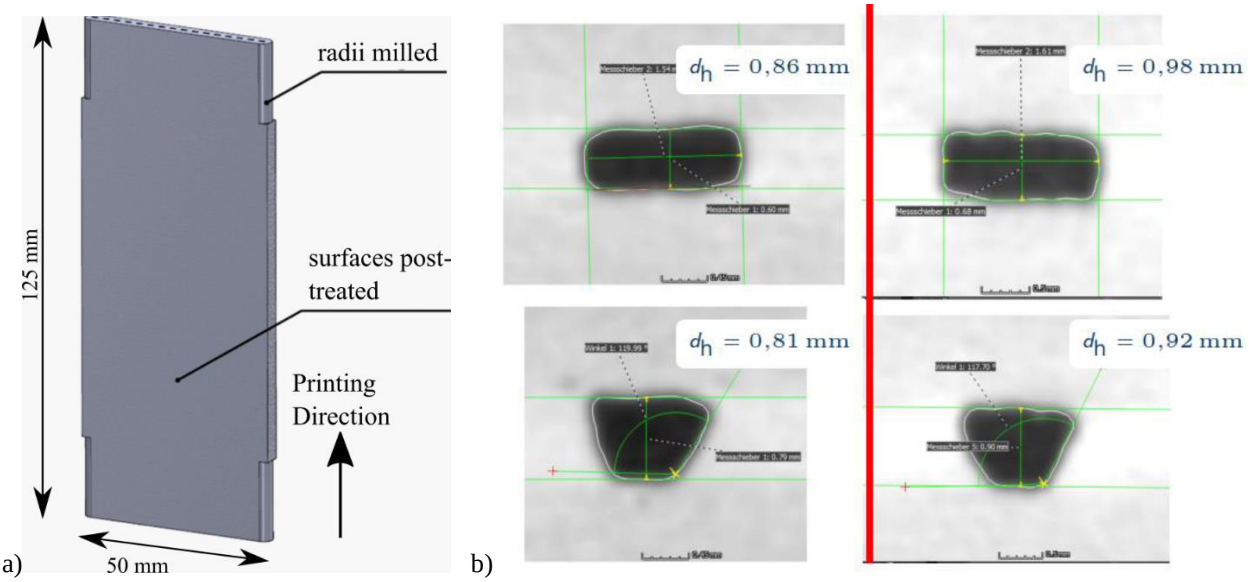

Figure 1 a): heat exchanger design and geometry; b): CT-Scan of different microchannels (K. Lemberg, T. Kramer, M. Raddatz & R. Barta, 2021)

Different channel geometries were also developed and tested to find out which channel geometry performs best and has the highest heat transfer. Since the process is a relatively new technology, validated construction methods often require an adaption to the SLM process. For example, the orientation of the body during the manufacturing process determines whether the manufacturing process can be used for the planned component or not. Also, overhangs can only be printed up to a certain angle and a maximum length without additional support material (Jacob C. Snyder et al., 2015). In microchannels the installation of these support structures is not possible. Therefore different post treatments and a clean up are necessary to improve imperfections. Targeted heat treatment not only reduces anisotropic component properties but also significantly increases thermal conductivity.

Additionally, the heat exchangers were examined through a non-destructive CT-scan. The result of these recordings are three-dimensional computer models of the heat exchanger, which can be freely moved, cut and geometrically measured in a similar way to a CAD system. In these models, imperfections such as blocked channels can be detected and the geometry can be checked so that exact heat transfer coefficients can be determined. The setpoint for each hydraulic diameter was $d_h = 0{,}75\ mm$. The actual hydraulic diameters were slightly different, as shown in Figure 1. The difference between the size of the rough channel surface and the smooth channel surface was also only observed through the CT-scan.

2.2 Measurement section

The additively manufactured heat exchanger is put in a so-called heat exchanger module (Figure 2), which is insulated and connected to the test stand. The temperature is measured on the surface of the heat exchanger and the heat load is applied through an electric resistance heater connected to the heat exchanger via a copper plate. In order to determine the heat transfer into the channel, it is necessary to determine the wall temperature inside the channel. Since a direct measurement is not possible due to the limited space in a microchannel without fundamentally distorting the flow, the outside temperature is measured on the contact side between the temperature measuring plate and the heat exchanger. Subsequently, assuming a one-dimensional heat conduction in the material and knowing the heat flow density of the heater, the temperature in the duct can be calculated. The inlet to the heat exchanger is improved by way of a venturi distributor. The test rig with its most important parts and measuring points is shown in Figure 3.

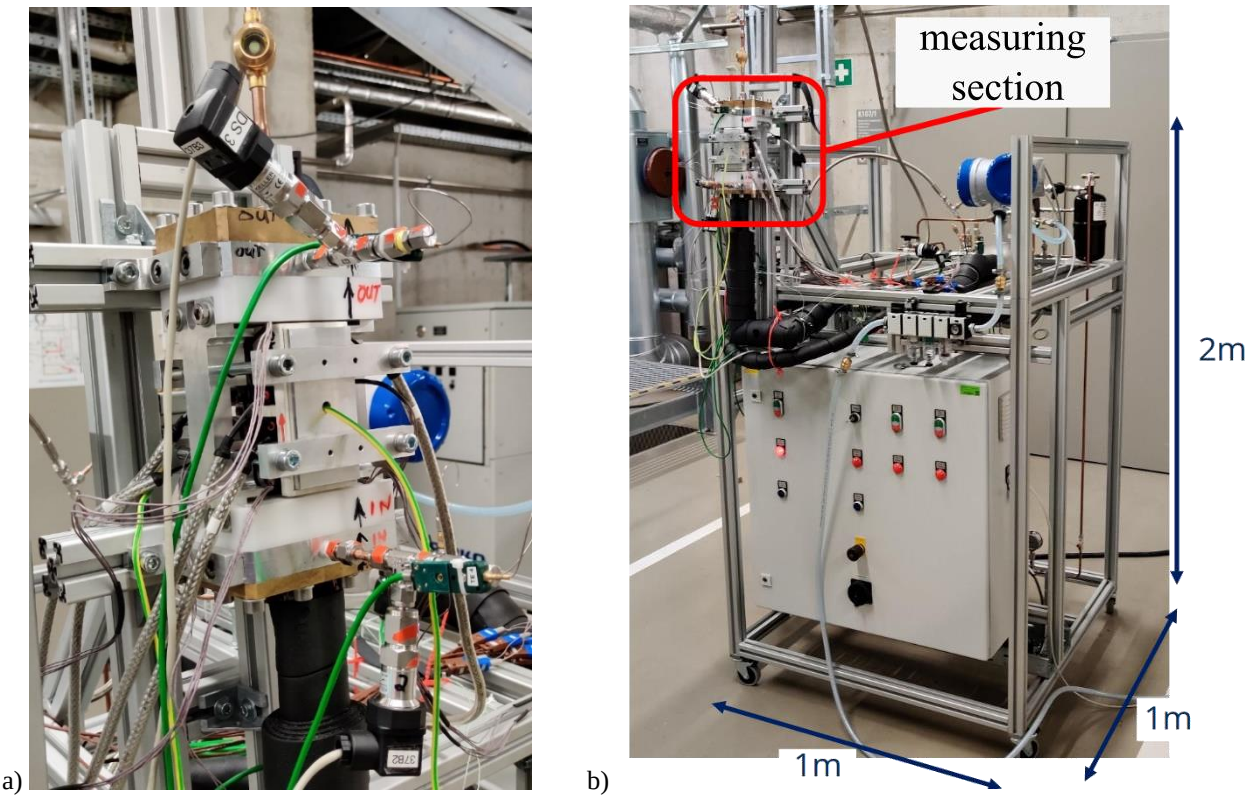

Figure 2: a): Heat exchanger module; b): Test stand with heat exchanger module (schematic in Figure 3) (K. Lemberg, T. Kramer, M. Raddatz & R. Barta, 2021)

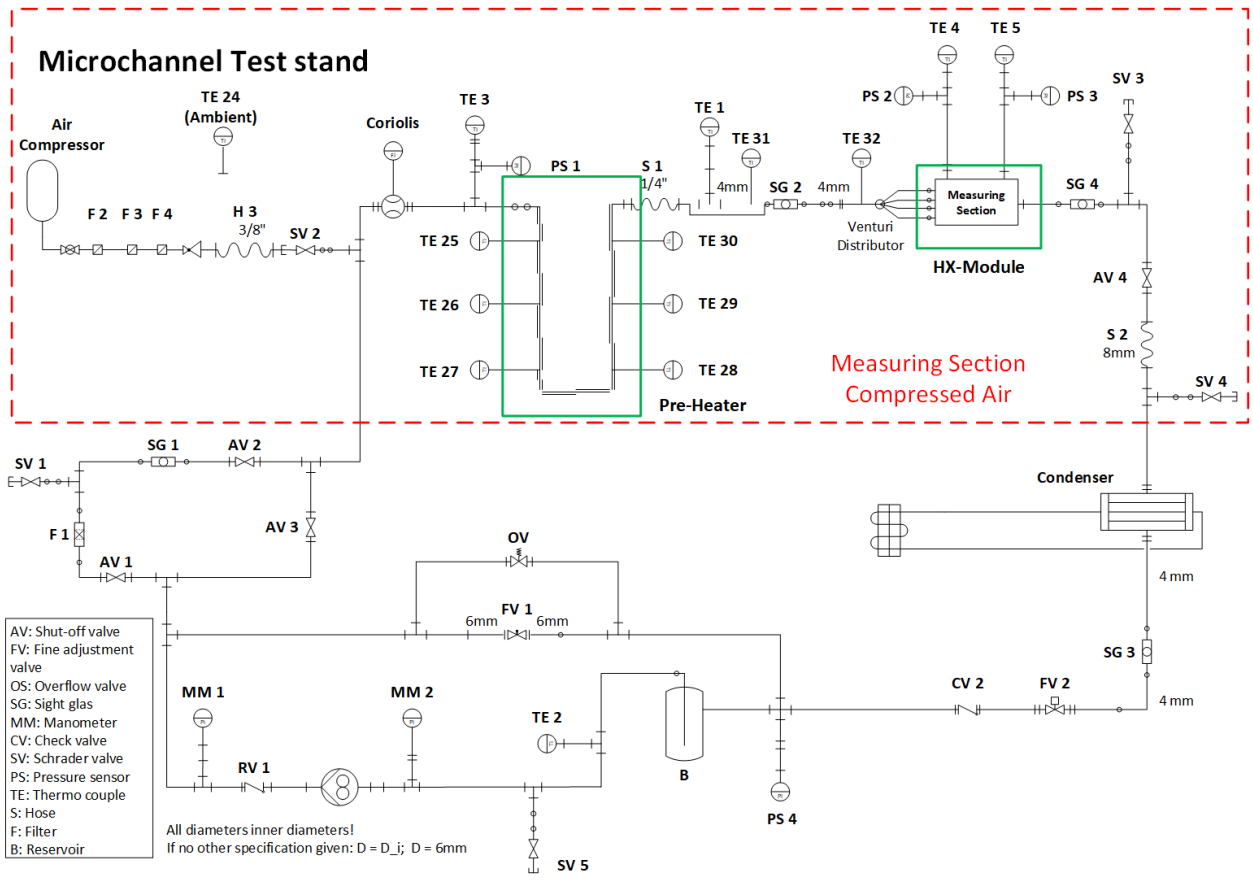

Figure 3: Schematic of the heat exchanger test stand (K. Lemberg, T. Kramer, M. Raddatz & R. Barta, 2021)

The test stand can be operated with different cooling fluids. Compressed air is provided at approximately 6 bar to compare the heat transfer performance of a two-phase fluid with a one-phase fluid. When using a two-phase fluid, the test rig is operated in a cooling cycle, where a pump pumps the liquid fluid to the heat exchanger module at the desired pressure. The fluid is pre heated in the section in front of the heat exchanger module and condensed to its initial temperature after the test section. Additionally, the heat exchanger module can be tilted up to an angle of 90°.

The measurements were performed as benchmark tests at a maximum surface temperature of 100 °C to simulate the maximum temperature of the IGBT and to be able to compare the performance of the different fluids and heat exchanger geometries. The hydrofluoroolefin (HFO)-refrigerant R1336mzz(Z) was used as the working fluid because of its nominal evaporating temperature, it being non-toxic and non-flammable and possessing a low global warming potential (GWP). Two different geometries with two surface roughnesses were tested and compared with each other as well as with the performance of a one-phase fluid. To be able to compare the heat transfer of the different geometries, the dimensionless Nu can also be calculated:

$$Nu = \frac{\alpha \cdot d_{\mathrm{h}}}{\lambda_{\mathrm{fluid}}} \tag{3}$$

The heat transfer coefficient α herein can be determined as follows:

$$\alpha = \frac{\dot{q}}{\vartheta_{\mathrm{channel}} - \vartheta_{\mathrm{fluid}}} \tag{4}$$

$\vartheta_{\mathrm{channel}}$ is the average temperature at the channel surface as described above, $\vartheta_{\mathrm{fluid}}$is the average temperature of the fluid and $\dot{q}$ describes the average heat flux from the heater to the fluid. In the described test stand configuration, the heat transfer coefficient and the Nusselt number can only be determined as an average over the heat exchanger because the local temperatures of the evaporating fluids and the local heat flux cannot be determined.

3. RESULTS

Figure 4 shows the Nusselt number of all measured refrigerant benchmark tests as a function of the mass flux. Up to a mass flow density referred to here as the critical mass flow density, the tests were run into the superheated range, since the heat transfer was high enough to absorb more heat than the enthalpy of vaporization of the fluid. The critical mass flow densities of the benchmark tests depend on the heat transfer coefficient and the actual mass flow, and are also different for the different geometries. They are shown in Table 1 together with the size of the cross section, the hydraulic diameter and the surface roughness.

Table 1: Geometric and experimental data of the tested heat exchangers

Heat exchanger channel geometry	**Cross section A_Q (all channels) [mm²]**	**Hydraulic diameter d_H [mm]**	**Surface roughness R_z [µm]**	**Critical mass flow density[$\frac{kg}{m^2 s}$]**
Trapezoidal, rough	13,6	0,92	100	490
Trapezoidal, smooth	10,1	0,81	40	660
Rectangular, rough	18,4	0,98	100	317
Rectangular, smooth	14,5	0,86	40	318

The inlet pressure is regulated to $p_{in} = 2\ bar$, the inlet vapor mass fraction is regulated to $x_{in} = 0$, the heater is regulated, so that the surface temperature of the heat exchanger has a maximum of $\vartheta_{SF,max} = 100$ °C and the mass flux is varied.

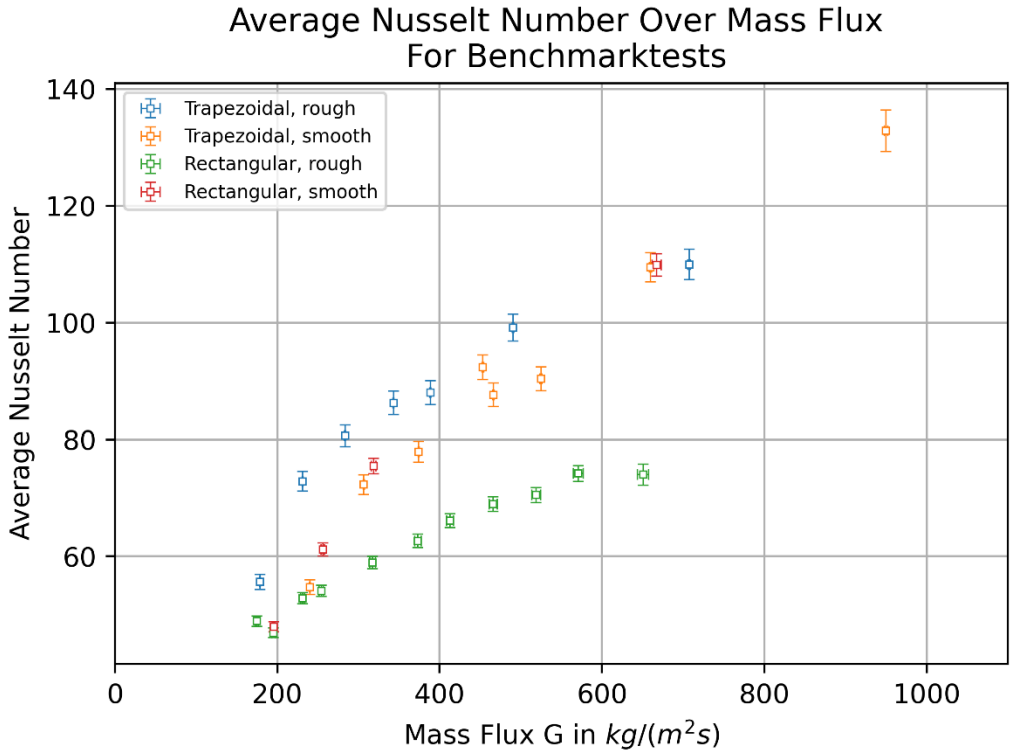

Figure 4: Average Nusselt number over mass flux for the benchmark tests of refrigerant R1336mzz(Z) and different heat exchanger-geometries (K. Lemberg, T. Kramer, M. Raddatz & R. Barta, 2021)

The benchmark test with the smooth trapeze geometry achieves the highest Nusselt number, while the benchmark test, using the rough rectangular geometry has the lowest Nusselt number.

Investigations revealed different approaches to flow patterns that could be assigned to the measured values. It seems that the roughness of the heat exchanger channels in this case leads to a decline of the heat transfer, contrary to the results of other literature. It is possible that the very high roughness of the walls causes the liquid film of the annular flow to break off and thus led to local hotspots. Figure 5 shows the heat loads transferred in the benchmarktests for the fluids air and R1336mzz(Z) using the different geometries. It can be shown that, by using an evaporating fluid, the heat transffered can be more than doubled for each geometry with two-phase cooling in comparison to cooling with air. The influence of the geometry on the heat transfer is higher when using a two-phase fluid than using a one-phase fluid.

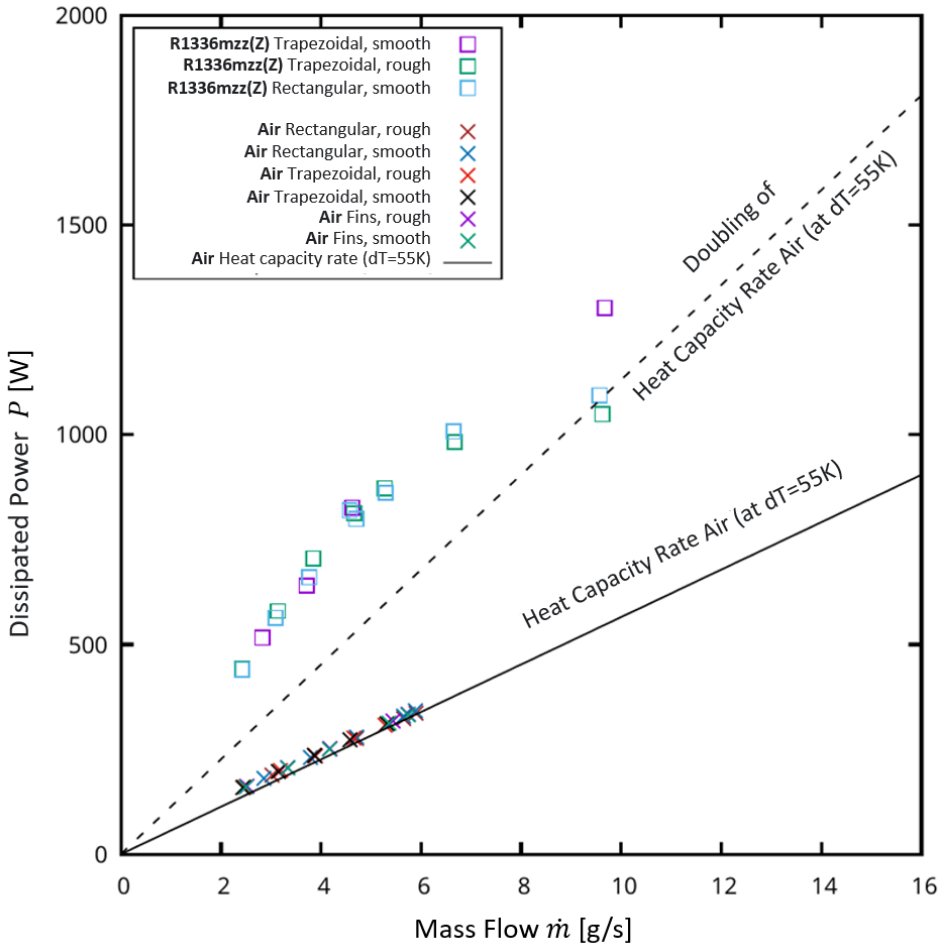

Figure 5: Heat load of benchmark tests for air and for refrigerant R1336mzz(Z) (K. Lemberg, T. Kramer, M. Raddatz & R. Barta, 2021)

In addition to the above described benchmark tests, measurements describing the influence of the vapor mass fraction on the heat transfer coefficient were done. Here for the inlet vapor mass fraction was varied, while the heat flux, the mass flow and the inlet pressure were held constant. Figure 6 shows the heat transfer coefficients for different inlet vapor mass fractions and the geometries rough trapezoid and rough rectangle. A maximum heat transfer coefficient of $\alpha = 6000\ \frac{W}{m^2K}$ for the rough trapezoidal geometry and $\alpha = 3450\ \frac{W}{m^2K}$ for the rough rectangular geometry can be observed at an inlet vapor mass fraction of $x_{\text{in}} \approx 0{,}55$. Although the type of flow cannot be precisely determined in the tests carried out in the project, it can be assumed that Taylor flow or ring flow is present in the area of optimum vapor mass fraction. At higher vapor mass fractions than the optimum the heat transfer coefficient falls rapidly.

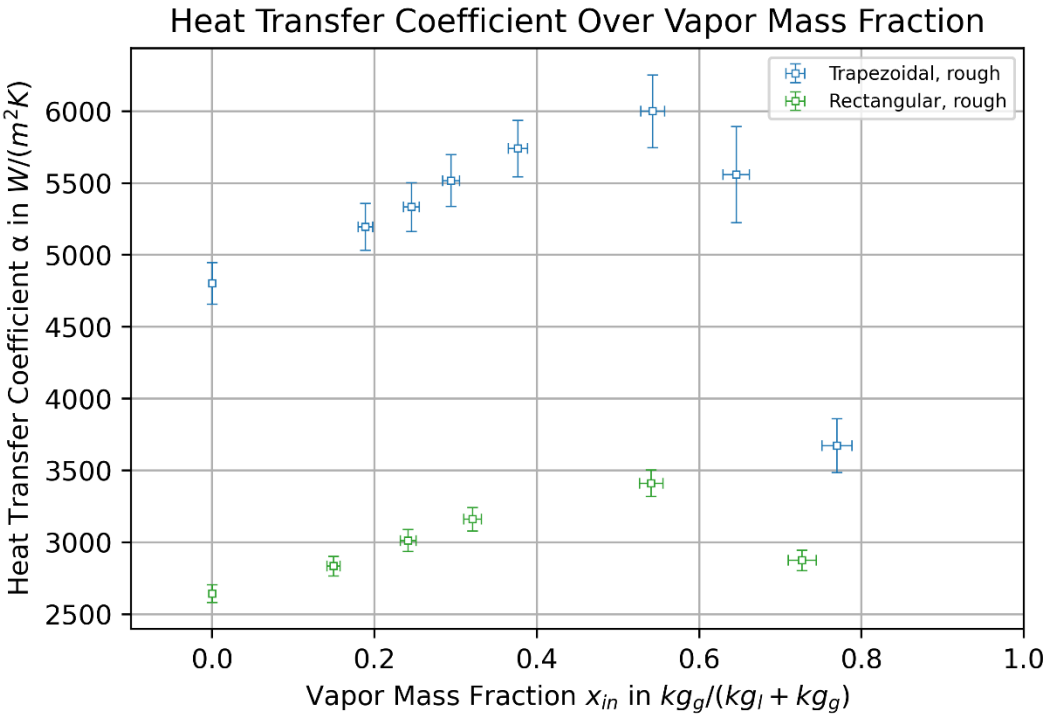

Figure 6: Heat transfer coefficient depending on inlet vapor mass fraction (K. Lemberg, T. Kramer, M. Raddatz & R. Barta, 2021)

To determine the inlet and outlet vapor mass fractions the heat loss across the preheater was taken into account and thoroughly examined, while the losses of the heat exchanger module were neglected. The high error bar is due to the low temperature differences between the heat exchanger module and the fluid.

3.1 Sources of Losses and Uncertainty Analysis

The errors, shown in figure 4 to figure 6 as error bars, were calculated using the Gaussian Propagation of uncertainty. Hereby the measuring errors shown in Table 2 were used.

Table 2: Summary of measurement uncertainty

Measurement	**Measurement Uncertainty**
Thermocouple, heat exchanger	$\Delta\vartheta_{\mathrm{SM}} = \mp 0{,}2\ K$
Thermocouple, fluid temperature	$\Delta\vartheta_{\mathrm{Fluid}} = \mp 0{,}1\ K$
Thermocouple, ambient air	$\Delta\vartheta_{\mathrm{a}} = \mp 0{,}1\ K$
Pressure	$\Delta p = \mp 0{,}25\% \cdot p$
Mass flow	$\Delta\dot{m} = \mp 0{,}25\% \cdot \dot{m}$
Electrical power	$\Delta P_{\mathrm{el}} = \mp 1{,}6\ \% \cdot P_{el}$
Cross section	$\Delta A_{\mathrm{Q}} = \mp 0{,}014\ mm^2$
Heat exchanger channels surface area	$\Delta A_{\mathrm{Channel}} = \mp 0{,}68\ cm^2$

The heat flow rate $\dot{Q}$ entering the fluid is determined by the electrical power. Since the sub-module is insulated and the exact determination of the heat loss is not possible, the dissipative heat loss is neglected in the shown results. The heat loss in the preheater is calculated by calculating the transmittance of the preheater to the ambient air in by measuring the difference of electrical power and enthalpy difference in the one-phase region.

4. CONCLUSIONS

This paper presented an experimental investigation comparing multiple additively-manufactured microchannel heat exchanger geometries using both single-phase and two-phase flow in a power electronics cooling application. The increase in heat transfer achieved with the two-phase cooling for the given geometries by a factor of about two (increase in the thermal conductivity element by more than 100%) compared to air shows that the increased electronic loads to be expected in the future can be managed without a significant increase or even with a reduction in size and weight of the heat exchanger. A constant challenge in the application of two-phase cooling in electronics still is the stability of boiling at different loads and surface temperatures. This challenge must be tackled by optimizing the system control and stability and by improving the predictions of the heat transfer coefficient depending on vapor mass fraction, geometry and mass flux, among other parameters. The additive manufacturing of microchannel heat exchangers has been improved and it was shown that thereby new and innovative geometries can be produced and tested. It was also shown that the exact hydraulic diameter needs to be determined after the production.
Additionally to the tested geometries "trapezoidal" and "rectangular" other geometries like "circular", "sinusoidal" or "star" could be measured for further investigations regarding the influence of the geometry. Also, further measurements are needed to develop general correlations for these microchannels.

NOMENCLATURE

Co	Confinement number	(-)
d_B	Bubble diameter	(m)
d_h	Hydraulic diameter	(m)
G	Mass flux	(kg/m^2)
Kn	Knudsen number	(-)
L	Representative physical length scale	(m)
$\dot{m}$	mass flow	(kg/s)
Nu	Nusselt number	(-)
p	pressure	(bar)
$\dot{Q}$	Heat flow	(W)
Re	Reynolds number	(-)
R_z	Surface roughness	(µm)
V	Volume	m^3
x	vapor mass fraction	(kg/kg)

Acronyms

CAD	Computer-aided design
CT	Computed tomography
GTO	Gate Turn Off
GWP	Global Warming Potential
HFO	Hydrofluoroolefine
HX	Heat exchanger
IGBT	Insulated Gate Bipolar Transistor
IGCT	Integrated Gate Commutated Thyristor
MOSFET	Metal Oxide Semiconductor Field Effect Transistor
SLM	Selective laser melting
SM	HX-Sub-Module
TE	Thermo couple

Greek Symbols

α	Heat transfer coefficient	(W/m^{2}K)
η	Efficiency	(-)
ϑ	Temperature	(°C)
λ	Thermal conductivity	(W/mK)
γ	Compactness performance factor	(-)

Subscript

a	Ambient
Comp	Compressor
in	Inlet
el	electrical
Exp	Expander
Q	Cross section
l	Liquid
log	Logarithmic
max	Maximum
min	Minimum
out	Outlet
SF	Surface
SM	HX-Sub-Module

References

Alexander Raabe. (2021). *Theoretische und experimentelle Untersuchung zu Wärmeübergangs- Druckverlust-Korrelationen beim Phasenwechsel in Microchannel-W.*

B. Jayant Baliga (2015). The IGBT Device: Physics, Design and Applications of the Insulated Gate Bipolar Transistor. *The IGBT Device: Physics, Design and Applications of the Insulated Gate Bipolar Transistor.* Advance online publication. https://doi.org/10.1016/C2012-0-02174-6

Dirk Herzog, Vanessa Seyda, Eric Wycisk, & Claus Emmelmann (2016). Additive manufacturing of metals. *Acta Materialia*, *117*, 371–392. https://doi.org/10.1016/j.actamat.2016.07.019

Eric M Smith. (2005). *Advances in Thermal Design of Heat Exchangers - A numerical approach: direct-sizing, step-wise rating and transients.*

Jacob C. Snyder, Curtis K. Stimpson, Karen A. Thole, & Dominic J. Mongillo (2015). Build Direction Effects on Microchannel Tolerance and Surface Roughness. *Journal of Mechanical Design*, *137*(11), 111411. https://doi.org/10.1115/1.4031071

K. Lemberg, T. Kramer, M. Raddatz & R. Barta. (2021). *Additiv gefertigte, hoch angepasste Micro-Channel Wärmeübertrager in einem hocheffizienten Kaltdampfkühlsystem für Flugzeug- Leistungselektronik.* Förderkennzeichen 20E1707 (LuFo V-3 Projekt).

Kuppan Thulukkanam. (2013). *Heat Exchanger Design Handbook, Second Edition (MECHANICAL ENGINEERING).*

Lubin Han, Lin Liang, Yong Kang, & Yufeng Qiu (2021). A Review of SiC IGBT: Models, Fabrications, Characteristics, and Applications. *IEEE Transactions on Power Electronics*, *36*(2), 2080–2093. https://doi.org/10.1109/TPEL.2020.3005940

Noriyuki Iwamuro, & Thomas Laska (2017). IGBT history, state-of-the-art, and future prospects. *IEEE Transactions on Electron Devices*, *64*(3), 741–752. https://doi.org/10.1109/TED.2017.2654599

S. Mostafa Ghiaasiaan (2007). Two-phase flow, boiling and condensation: In conventional and miniature systems. *Two-Phase Flow, Boiling and Condensation: In Conventional and Miniature Systems*, *9780521882*. https://doi.org/10.1017/CBO9780511619410

Satish G. Kandlikar (2002). Fundamental issues related to flow boiling in minichannels and microchannels. *Experimental Thermal and Fluid Science*, *26*(2-4), 389–407. https://doi.org/10.1016/S0894-1777(02)00150-4

T. G. Karayiannis, & M. M. Mahmoud (2017). Flow boiling in microchannels: Fundamentals and applications. *Applied Thermal Engineering*, *115*, 1372–1397. https://doi.org/10.1016/j.applthermaleng.2016.08.063

ACKNOWLEDGEMENT

We would like to thank everyone who worked on the corresponding project, especially Benedikt Bederna and Professor Gampe.

The authors, most importantly acknowledge the financial support by the Federal Ministry of Economic Affairs and Energy (funding indicator 20E1707).